Published in final edited form as:
Science. 2014 December 5; 346(6214): 1234–1238. doi:10.1126/science.1256478.

Neutrophils scan for activated platelets to initiate inflammation

Vinatha Sreeramkumar[1], **José M. Adrover**[1], **Ivan Ballesteros**[2], **Maria Isabel Cuartero**[2], **Jan Rossaint**[3], **Izaskun Bilbao**[1,4], **Maria Nácher**[1,5], **Christophe Pitaval**[1], **Irena Radovanovic**[1], **Yoshinori Fukui**[6], **Rodger P. McEver**[7], **Marie-Dominique Filippi**[8], **Ignacio Lizasoain**[2], **Jesús Ruiz-Cabello**[1,4], **Alexander Zarbock**[3], **María A. Moro**[2], and **Andrés Hidalgo**[1,9,*]

[1] Department of Epidemiology, Atherothrombosis and Imaging, Centro Nacional de Investigaciones Cardiovasculares (CNIC), Madrid, Spain.

[2] Unidad de Investigación Neurovascular, Deparment of Pharmacology, Faculty of Medicine, Universidad Complutense and Instituto de Investigación Hospital 12 de Octubre (i+12), Madrid, Spain

[3] Department of Anesthesiology and Critical Care Medicine, University of Münster and Max Planck Institute Münster, Münster, Germany.

[4] Ciber de Enfermedades Respiratorias (CIBERES), Madrid, Spain.

[5] Faculty of Science, Medicine and Health, University of Wollongong, New South Wales, Australia.

[6] Division of Immunogenetics, Department of Immunobiology and Neuroscience, Kyushu University, Japan.

[7] Cardiovascular Biology Research Program, Oklahoma Medical Research Foundation, Oklahoma City, OK.

[8] Division of Experimental Hematology and Cancer Biology, Cincinnati Children's Research Foundation, University of Cincinnati College of Medicine, Cincinnati, OH, USA.

[9] Institute for Cardiovascular Prevention, Ludwig-Maximilians-University, Munich, Germany.

Abstract

Immune and inflammatory responses require leukocytes to migrate within and through the vasculature, a process that is facilitated by their capacity to switch to a polarized morphology with asymmetric distribution of receptors. We report that neutrophil polarization within activated venules served to organize a protruding domain that engaged activated platelets present in the bloodstream. The selectin ligand PSGL-1 transduced signals emanating from these interactions, resulting in redistribution of receptors that drive neutrophil migration. Consequently, neutrophils unable to polarize or to transduce signals through PSGL-1 displayed aberrant crawling, and blockade of this domain protected mice against thrombo-inflammatory injury. These results reveal

[*]Correspondence: ahidalgo@cnic.es Department of Epidemiology, Atherothrombosis and Imaging, Centro Nacional de Investigaciones Cardiovasculares (CNIC), Melchor Fernández Almagro 3, 28029 Madrid, Spain. Phone: +34 91 4531200 (Ext. 1504). Fax: +34 91 4531245.

The authors declare no other conflicts of interest.

that recruited neutrophils scan for activated platelets, and suggest that their bipolarity allows integration of signals present at both the endothelium and the circulation before inflammation proceeds.

Neutrophils are primary effectors of the immune response against invading pathogens, but are also central mediators of inflammatory injury (1). Both functions rely on their remarkable ability to migrate within and through blood vessels. Migration of neutrophils is initiated by tethering and rolling on inflamed venules, a process mediated by endothelial selectins (2). Selectin- and chemokine-triggered activation of integrins then allows firm adhesion, after which leukocytes actively crawl on the endothelium before they extravasate or return to the circulation (3). A distinct feature of leukocytes recruited to inflamed vessels is the rapid shift from a symmetric morphology into a polarized form in which intracellular proteins and receptors rapidly segregate (4). In this way neutrophils generate a moving front or leading edge where the constant formation of lamellipodia (actin projections) guides movement, and a uropod or trailing edge where highly glycosylated receptors accumulate (5, 6). We deemed unlikely that this dramatic reorganization served to exclusively generate a front-to-back axis for directional movement, and explored the possibility that neutrophil polarization functions as an additional checkpoint during inflammation.

We performed intravital microscopy (IVM) imaging of venules in cremaster muscles of mice treated with the cytokine tumor necrosis factor α (TNFα), an inflammatory model in which the vast majority of recruited leukocytes are neutrophils (Figure S1). Within seconds after arresting, leukocytes formed a lamellipodia-rich domain, or leading edge, and a CD62L-enriched uropod, which we could identify by its localization opposite to the leading edge and the direction of cell movement (Movie S1 and Figure 1A) (6-8). Confirming previous reports we observed numerous interactions of platelets with the leading edge of adherent neutrophils (Figure 1A and Figure S2A; and (8-10)). During these experiments we noticed that the uropod underwent continuous collisions with circulating platelets, a fraction of which established measurable interactions that were usually transient (Figure 1B and Movie S2). Because platelets captured by the uropod represented a substantial fraction of all interactions (31%), we searched for the receptor(s) mediating these contacts. We reasoned that PSGL-1, a glycoprotein ligand for P-selectin (11) that segregates to the uropod of polarized neutrophils (12), could be responsible for these interactions. Analysis of mice deficient in PSGL-1 (*Selplg*$^{-/-}$ mice) revealed marked reductions in platelet interactions with the uropod, whereas those at the leading edge remained unaffected (Figure 1B). In contrast, deficiency in the β2 integrin Mac-1 (*Itgam*$^{-/-}$) resulted in reductions at both the uropod and leading edge (Figure 1B). *In vivo* labeling of Mac-1 and PSGL-1 confirmed these functional data, with Mac-1 localized throughout the cell body and PSGL-1 exclusively at the uropod (Figure 1C). Specifically, PSGL-1 clustered in a small region of the uropod, whereas CD62L was widely distributed in this domain (Figure 1C). Analyses of mice expressing a functional Dock2-GFP protein, a guanine nucleotide exchange factor of Rac GTPases (13), revealed co-localization of Dock2 with PSGL-1 clusters on crawling neutrophils (Figure S3 and Movie S3), suggesting active structural dynamics within this region. This observation together with the high frequency of platelet collisions with the PSGL-1 clusters suggested that this domain might be actively protruding into the vessel lumen. Using high-speed

spinning-disk IVM we could obtain three-dimensional reconstructions of polarized neutrophils within inflamed venules of Dock2-GFP mice (Figure 1D) demonstrating that the PSGL-1 clusters indeed projected towards the vessel lumen in about 40% of adherent neutrophils, while in the remaining 60% of the cells it extended laterally, parallel to the endothelial surface (Figure 1D-E and Movie S4). As a consequence, the luminal space of inflamed venules was populated by multiple PSGL-1-bearing clusters suitably positioned to interact with circulating cells (Figure 1F and Movie S5).

The observation that only a small fraction of circulating platelets engaged in interactions with the uropod prompted us to search for "subsets" of platelets prone to this behavior. *In vivo* labeling for P-selectin or for active β3 integrins revealed that virtually all platelets interacting with the uropod were activated (P-selectin^{+} or with active β3-integrins), whereas a fraction of those engaging the leading edge were not (Figure 1G and Figures S2B and S4). These findings further suggested that P-selectin present on the surface of activated platelets might be mediating the interactions with the PSGL-1 clusters. Analyses of mice deficient in P-selectin (*Selp*$^{-/-}$ mice) indeed demonstrated patterns of platelet interactions with the two leukocyte subdomains that were similar to those found in mice lacking PSGL-1 (Figure 1B). These results indicated that neutrophils recruited to inflamed vessels extend a PSGL-1-bearing microdomain into the vessel lumen that "scans" for activated platelets present in the bloodstream through P-selectin.

During the course of our IVM experiments we also noticed alterations in the intravascular behavior of adherent neutrophils in the different mutant mice. Deficiency in Mac-1 severely compromised neutrophil crawling on the inflamed vasculature (Figure 2A-B), a process previously reported to be mediated by this integrin (3). Surprisingly, although PSGL-1 was excluded from the area of contact with the endothelium (Figure 1D-E), neutrophils deficient in this glycoprotein also displayed reductions in crawling displacement and velocity (Figure 2A-B), and these defects were cell-intrinsic (Figure S5 and Movie S6). To exclude potential defects originating from PSGL-1 contributions in the early steps of leukocyte recruitment by binding endothelial P-selectin (14), we prevented PSGL-1 binding to P-selectin using a blocking antibody injected after neutrophils had adhered. Inhibition at this stage did not affect leukocyte adhesion to inflamed venules but specifically decreased interactions with the uropod (Figure S6) and caused reductions in crawling kinetics (Figure 2A-B). We thus speculated that engagement of PSGL-1 at the uropod might promote crawling of polarized neutrophils. To test this hypothesis we first induced transient depletion of platelets, a treatment that resulted in virtual suppression of crawling (Figure 2A-B and Figure S7A). We next analyzed two models in which neutrophil polarization or signaling through PSGL-1 was impaired. In the first model we induced hematopoietic-specific deletion of the gene encoding Cdc42 (Figure S8A), a small Rho-GTPase required for neutrophil polarization (15). Confirming previous *in vitro* observations, Cdc42-deficient neutrophils were unable to form a leading edge-to-uropod axis and instead formed multiple protrusions, lacked a distinguishable uropod, and failed to form PSGL-1 clusters *in vivo* (Figure S8B). Impaired polarization in these mutants compromised interactions between neutrophils and circulating platelets (Figure S8C), and neutrophils in these mice displayed severely impaired crawling kinetics (Figure 2C-D). In the second model we analyzed mice in which PSGL-1 is normally

distributed at the cell surface and can interact with P-selectin but cannot propagate outside-in signals due to the absence of the cytoplasmic domain (PSGL-1$^{\Delta Cyt}$ mice; (16)). Although neutrophil adhesion to TNFα-stimulated vessels was partially compromised in PSGL-1$^{\Delta Cyt}$ mice due to reductions in the surface levels of PSGL-1, those cells that adhered polarized normally (Figure S9A) and displayed marked reductions in crawling kinetics (Figure 2C-D) despite elevated levels of Mac-1 on the surface (Figure S9B). Thus, polarization of a signaling-competent PSGL-1 drives intravascular migration of neutrophils.

To search for possible mechanisms by which PSGL-1-derived signals promoted crawling, we analyzed the *in vivo* distribution of Mac-1 and the chemokine receptor CXCR2, two receptors required for intravascular migration of neutrophils (3, 17). In wild-type cells, Mac-1 was homogeneously distributed throughout the cell body whereas CXCR2 preferentially localized at the leading edge (Figure 2E and Movie S7). Remarkably, neutrophils deficient in PSGL-1 exhibited a mislocalization of both receptors (Figure 2E, Figure S10 and Movie S8). These alterations were even more dramatic in wild-type mice upon platelet depletion (Figures S7B, S10, and Movie S9), which agreed with the suppression of crawling in these mice (Figure 2A). Interestingly, absence or inhibition of PSGL-1 in Mac-1-deficient mice did not lead to further reductions in platelet interactions or crawling kinetics (Figure S11), indicating that these receptors function along the same pathway and that additional platelet-derived mediators and unknown neutrophil receptors that mediate platelet interactions can regulate crawling. Thus, intact distribution of and signaling through PSGL-1 at the uropod regulates neutrophil crawling, at least in part by orchestrating the appropriate distribution of adhesive and chemotactic receptors.

We next explored how this phenomenon might contribute to pathogenic inflammation. We used a model of acute lung injury (ALI) in Balb/c mice that closely simulates transfusion-related ALI (18). In this model, transient elimination of neutrophils or platelets protects from death (Figure 3A and (19)), indicating that this might be an appropriate model to study the functional partnership between these cells. Intravital analyses of the cremaster microvessels in ALI-induced mice confirmed the findings in crawling kinetics, receptor distribution and luminal or lateral projections made using TNFα (Figure S12 and Movie S10), and further revealed that during ALI the uropod becomes the predominant domain for platelet interactions, which contrasted with the preferred use of the leading edge in the non-pathogenic TNFα-induced model (Figure 3B-C). Interactions at the uropod during ALI were mediated by PSGL-1, whereas Mac-1 mediated interactions with both domains (Figure 3C and Figure S13). We obtained similar responses in a model of endotoxemia, (Figure 3D), indicating that during pathological inflammation the uropod becomes the dominant interacting domain for circulating platelets.

To test whether engagement of PSGL-1 at the uropod were causally related to neutrophil-mediated vascular inflammation, we explored their contribution in the model of ALI. Intravital imaging of the pulmonary microcirculation revealed a rapid increase in platelets captured by recruited neutrophils that were strongly inhibited by blocking PSGL-1 (Figure S14). In addition, deficiency in PSGL-1 or Mac-1, or inhibition of PSGL-1, resulted in moderate protection from ALI-induced death (Figure 4A and Figure S15A). Use of computed tomography to track pulmonary edema over time revealed partial protection from

ALI in mice deficient in Mac-1 and almost complete protection when PSGL-1 interactions were blocked (Figure 4B-C). This protection correlated with reduced neutrophil infiltrates in lung (Figure S16) and suggested that interactions at the uropod critically contribute to vascular injury. Deficiency in either receptor or inhibition of PSGL-1 also prevented hepatic damage during endotoxemia (Figure 4D and Figure S15B). Consistent with previous reports (20, 21) we detected elevations in the plasma levels of neutrophil-derived extracellular traps (NETs) during ALI and sepsis. These elevations were completely blunted when platelets were depleted, by blocking PSGL-1, or in the absence of Mac-1 (Figure S17), suggesting that other forms of neutrophil activation can be triggered upon platelet interactions through PSGL-1.

Finally, we examined whether PSGL-1-mediated interactions also underlie ischemic injury, a prevalent form of vascular disease (22). We used a model of stroke triggered by permanent occlusion of the middle cerebral artery, in which neutrophil depletion significantly reduces tissue death as measured by the percentage of infarcted hemisphere (Figure S18 and (23)). Interactions between neutrophils and platelets within the microvasculature of infarcted brains were inhibited by blocking PSGL-1 (Figure 4E and Figure S19), and this correlated with significant reductions in infarct volumes when PSGL-1 was inhibited or in the absence of Mac-1 (Figure 4F).

We have uncovered a critical checkpoint during the early stages of inflammation; neutrophils recruited to injured vessels extend a domain into the lumen where PSGL-1 clusters scan for the presence of activated platelets. Only when productive interactions occur do neutrophils organize additional receptors needed for intravascular migration or generate NETs, and inflammation ensues (Figure S20 and Movie S11). Our findings reveal that the dynamic reorganization of neutrophil domains and receptors allows simultaneous interactions with both the vascular wall and activated platelets in the circulation to provide a rapid and efficient regulatory mechanism early during inflammation.

Supplementary Material

Refer to Web version on PubMed Central for supplementary material.

Acknowledgments

We thank G. Crainiciuc, J. A. Quintana, I. Ortega and A. Santos, for technical support and D. Sancho and S. González for insightful comments. The data presented in this manuscript can be found in the main paper and Supplemental Materials. This study was supported by NIH grants HL03463, HL085607 (to R.P.M.), and HL090676 (M.D.F.); German Research Foundation grants ZA428/8-1, ZA428/6-1 and SFB 1009-TP A05 (A.Z.); FP7 Marie Curie (ITN-264864; π-net) and S2010/BMD-2326 from Comunidad de Madrid (J.R-C.); Grants-in-Aid for Scientific Research from the Japan Society for the Promotion of Science (Y.F.); CSD2010-00045 and SAF2012-33216 from MINECO and S2010/BMD-2336 from Comunidad de Madrid (M.A.M.); Ramón y Cajal Fellowship (RYC-2007-00697), SAF2009-11037 and 2012-31142 from MINECO, S2010/BMD-2314 from Comunidad de Madrid, and 246655 from FP7-People-IRG Program (A.H.). The CNIC is supported by the MINECO and the Pro-CNIC Foundation. R.P.M. is co-founder of Selexys Pharmaceuticals Corp. which is developing monoclonal antibodies to PSGL-1 and P-selectin to treat inflammatory and thrombotic diseases. A patent application for the blockade of PSGL-1 in thrombo-inflammation has been filed by V.S. and A.H. (EP14382425.8).

References and Notes

1. Phillipson M, Kubes P. The neutrophil in vascular inflammation. Nat Med. 2011; 17:1381–1390. [PubMed: 22064428]
2. Ley K, Laudanna C, Cybulsky MI, Nourshargh S. Getting to the site of inflammation: the leukocyte adhesion cascade updated. Nat Rev Immunol. 2007; 7:678–689. [PubMed: 17717539]
3. Phillipson M, et al. Intraluminal crawling of neutrophils to emigration sites: a molecularly distinct process from adhesion in the recruitment cascade. J Exp Med. 2006; 203:2569–2575. [PubMed: 17116736]
4. Swaney KF, Huang CH, Devreotes PN. Eukaryotic chemotaxis: a network of signaling pathways controls motility, directional sensing, and polarity. Annu Rev Biophys. 2010; 39:265–289. [PubMed: 20192768]
5. Ridley AJ, et al. Cell migration: integrating signals from front to back. Science. 2003; 302:1704–1709. [PubMed: 14657486]
6. Sanchez-Madrid F, Serrador JM. Bringing up the rear: defining the roles of the uropod. Nat Rev Mol Cell Biol. 2009; 10:353–359. [PubMed: 19373240]
7. For more details on this and other procedures please refer to the Materials and Methods section in the Supplemental Materials.
8. Hidalgo A, et al. Heterotypic interactions enabled by polarized neutrophil microdomains mediate thromboinflammatory injury. Nat Med. 2009; 15:384–391. [PubMed: 19305412]
9. Semple JW, Italiano JE Jr. Freedman J. Platelets and the immune continuum. Nat Rev Immunol. 2011; 11:264–274. [PubMed: 21436837]
10. von Bruhl ML, et al. Monocytes, neutrophils, and platelets cooperate to initiate and propagate venous thrombosis in mice in vivo. J Exp Med. 2012; 209:819–835. [PubMed: 22451716]
11. Moore KL, et al. P-selectin glycoprotein ligand-1 mediates rolling of human neutrophils on P-selectin. J Cell Biol. 1995; 128:661–671. [PubMed: 7532174]
12. Chiang EY, Hidalgo A, Chang J, Frenette PS. Imaging receptor microdomains on leukocyte subsets in live mice. Nat Methods. 2007; 4:219–222. [PubMed: 17322889]
13. Kunisaki Y, et al. DOCK2 is a Rac activator that regulates motility and polarity during neutrophil chemotaxis. J Cell Biol. 2006; 174:647–652. [PubMed: 16943182]
14. Zarbock A, Ley K, McEver RP, Hidalgo A. Leukocyte ligands for endothelial selectins: specialized glycoconjugates that mediate rolling and signaling under flow. Blood. 2011; 118:6743–6751. [PubMed: 22021370]
15. Szczur K, Zheng Y, Filippi MD. The small Rho GTPase Cdc42 regulates neutrophil polarity via CD11b integrin signaling. Blood. 2009; 114:4527–4537. [PubMed: 19752396]
16. Miner JJ, et al. Separable requirements for cytoplasmic domain of PSGL-1 in leukocyte rolling and signaling under flow. Blood. 2008; 112:2035–2045. [PubMed: 18550846]
17. McDonald B, et al. Intravascular danger signals guide neutrophils to sites of sterile inflammation. Science. 2010; 330:362–366. [PubMed: 20947763]
18. Looney MR, Gilliss BM, Matthay MA. Pathophysiology of transfusion-related acute lung injury. Curr Opin Hematol. 2010; 17:418–423. [PubMed: 20601870]
19. Looney MR, et al. Platelet depletion and aspirin treatment protect mice in a two-event model of transfusion-related acute lung injury. J Clin Invest. 2009; 119:3450–3461. [PubMed: 19809160]
20. Caudrillier A, et al. Platelets induce neutrophil extracellular traps in transfusion-related acute lung injury. J Clin Invest. 2012; 122:2661–2671. [PubMed: 22684106]
21. Clark SR, et al. Platelet TLR4 activates neutrophil extracellular traps to ensnare bacteria in septic blood. Nat Med. 2007; 13:463–469. [PubMed: 17384648]
22. Donnan GA, Fisher M, Macleod M, Davis SM. Stroke. Lancet. 2008; 371:1612–1623. [PubMed: 18468545]
23. Cuartero MI, et al. N2 neutrophils, novel players in brain inflammation after stroke: modulation by the PPARgamma agonist rosiglitazone. Stroke. 2013; 44:3498–3508. [PubMed: 24135932]

24. Faust N, Varas F, Kelly LM, Heck S, Graf T. Insertion of enhanced green fluorescent protein into the lysozyme gene creates mice with green fluorescent granulocytes and macrophages. Blood. 2000; 96:719–726. [PubMed: 10887140]

25. Casanova-Acebes M, et al. Rhythmic modulation of the hematopoietic niche through neutrophil clearance. Cell. 2013; 153:1025–1035. [PubMed: 23706740]

26. Chevre R, et al. High-resolution imaging of intravascular atherogenic inflammation in live mice. Circ Res. 2014; 114:770–779. [PubMed: 24366169]

27. Wong CH, Jenne CN, Petri B, Chrobok NL, Kubes P. Nucleation of platelets with blood-borne pathogens on Kupffer cells precedes other innate immunity and contributes to bacterial clearance. Nat Immunol. 2013; 14:785–792. [PubMed: 23770641]

28. Rossaint J, et al. Synchronized integrin engagement and chemokine activation is crucial in neutrophil extracellular trap-mediated sterile inflammation. Blood. 2014; 123:2573–2584. [PubMed: 24335230]

29. Looney MR, et al. Stabilized imaging of immune surveillance in the mouse lung. Nat Methods. 2011; 8:91–96. [PubMed: 21151136]

One Sentence Summary

Neutrophils sample platelets in the bloodstream before initiating inflammation.

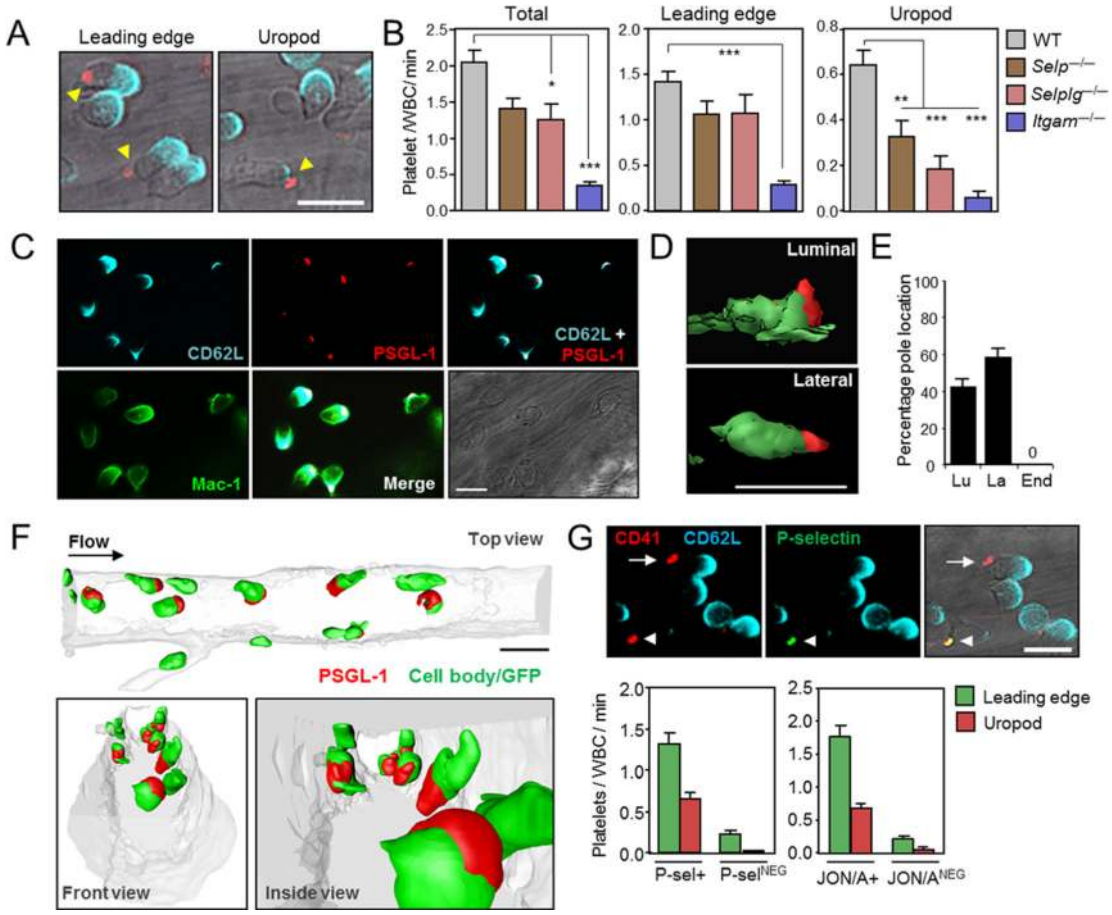

Figure 1. Neutrophils recruited to inflamed venules interact with activated platelets via protruding PSGL-1 clusters

(**A**) Micrographs of polarized neutrophils interacting with platelets (red; yellow arrowheads) through the leading edge or the CD62L-labeled uropod (blue). (**B**) Quantification of total or domain-specific platelet interactions in wild-type mice or mice deficient in P-selectin (*Selp*$^{-/-}$), PSGL-1 (*Selplg*$^{-/-}$) or Mac-1 (*Itgam*$^{-/-}$); n=5-8 mice, 38-133 interactions. (**C**) *In vivo* receptor distribution on polarized wild-type neutrophils. (**D**) Examples of luminal and lateral projections from 3D reconstructions of polarized Dock2-GFP neutrophils (see also Movie S4). (**E**) Frequency of neutrophils extending PSGL-1 clusters into the lumen (Lu), laterally (La) or between the cell body and the endothelium (En). n= 6 mice, 251 cells. (**F**) 3D reconstructions of an inflamed vessel showing the distribution of PSGL-1 clusters (see Movie S5). (**G**) Representative micrographs of neutrophils interacting with non-activated (arrow) or activated P-selectin+ platelets (arrowhead); and quantification of interactions of each domain with P-selectin+ or JON/A+ platelets. n=3-4 mice, 66-116 interactions. Scale bars, 10 μm. Bars show mean ± SEM. *, p<0.05; ***, p<0.001, one-way ANOVA analysis with Tukey's post-hoc test.

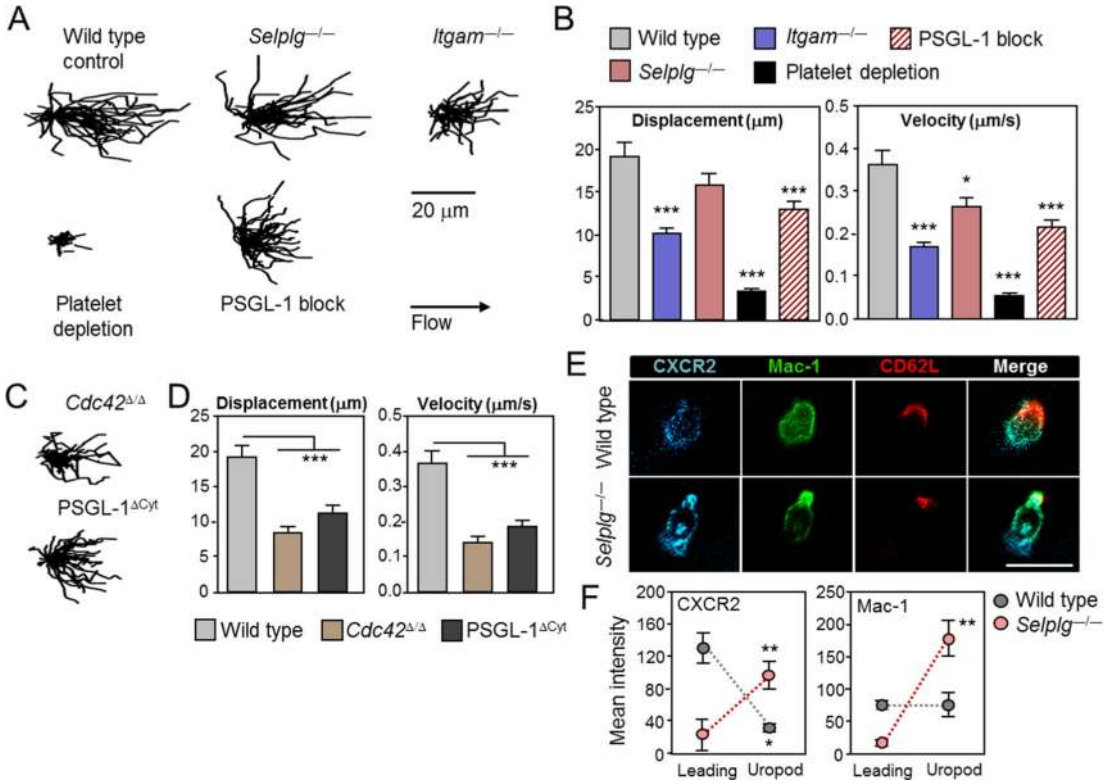

Figure 2. PSGL-1 controls intravascular motility and the distribution of Mac-1 and CXCR2

(**A**) Tracks of crawling neutrophils within inflamed vessels in untreated wild-type mice, mice deficient in PSGL-1 (*Selplg*$^{-/-}$) or Mac-1 (*Itgam*$^{-/-}$), and mice depleted of platelets using anti-platelet serum or treated with a PSGL-1-blocking antibody. (**B**) Quantification of the crawling displacements and instantaneous velocities of neutrophils in the same groups as (A); n=50-56 cells, 4-9 mice. (**C**) Tracks of neutrophils with conditional deletion of *Cdc42* or expressing a mutant form of PSGL-1 that lacks the cytoplasmic tail (PSGL-1$^{\Delta Cyt}$), and (D) quantification of the displacement per minute and instantaneous velocities of adhered neutrophils. n=50-55 cells, 3-5 mice. (**E**) Representative micrographs and quantification (**F**) of the *in vivo* distribution of CXCR2 and Mac-1 in polarized neutrophils from wild-type and PSGL- 1-deficient mice; n=17-19 cells, 3 mice. Scale bar, 10 μm. Data show mean ± SEM. *, p<0.05; **, p<0.01; ***, p<0.001; ANOVA with Tukey's multigroup test (B) or unpaired t-test (F).

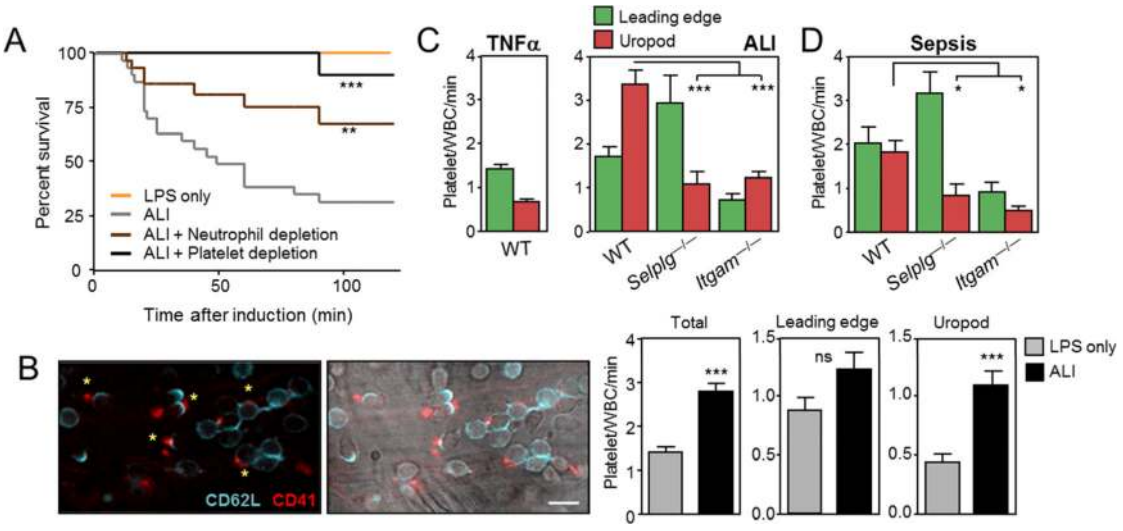

Figure 3. PSGL-1 at the uropod becomes a preferred docking site for platelets during pathological inflammation

(**A**) Survival curves of Balb/c mice treated with LPS alone or LPS plus anti-MHC-I to induce ALI. Neutrophils were depleted using anti-Ly6G and platelets using anti-platelet serum prior to induction of ALI. n=5-20 mice. (**B**) Left: representative micrographs of inflamed venules during ALI Asterisk indicates platelets interacting with the uropod of neutrophils. Right: quantification of platelet interactions with the leading edge or uropod in control (LPS only) and ALI-induced mice. Scale bar, 10 μm. n=3-4 mice, 32-73 interactions. (**C**) Frequency of interactions with the leading edge or uropod in TNFα-treated or ALI-induced mice, and distribution of interactions in WT mice, and mice deficient in PSGL-1 (*Selplg*$^{-/-}$) or Mac-1 (*Itgam*$^{-/-}$). n=3-5 mice, 23-137 interactions. (**D**) Frequency of interactions with the leading edge or uropod during sepsis in WT mice, and mice deficient in PSGL-1 or Mac-1. n= 3- 4 mice, 32-56 interactions. Bars show mean ± SEM. *, p<0.05; ***, p<0.001 as determined by ANOVA analysis with Tukey's multigroup test.

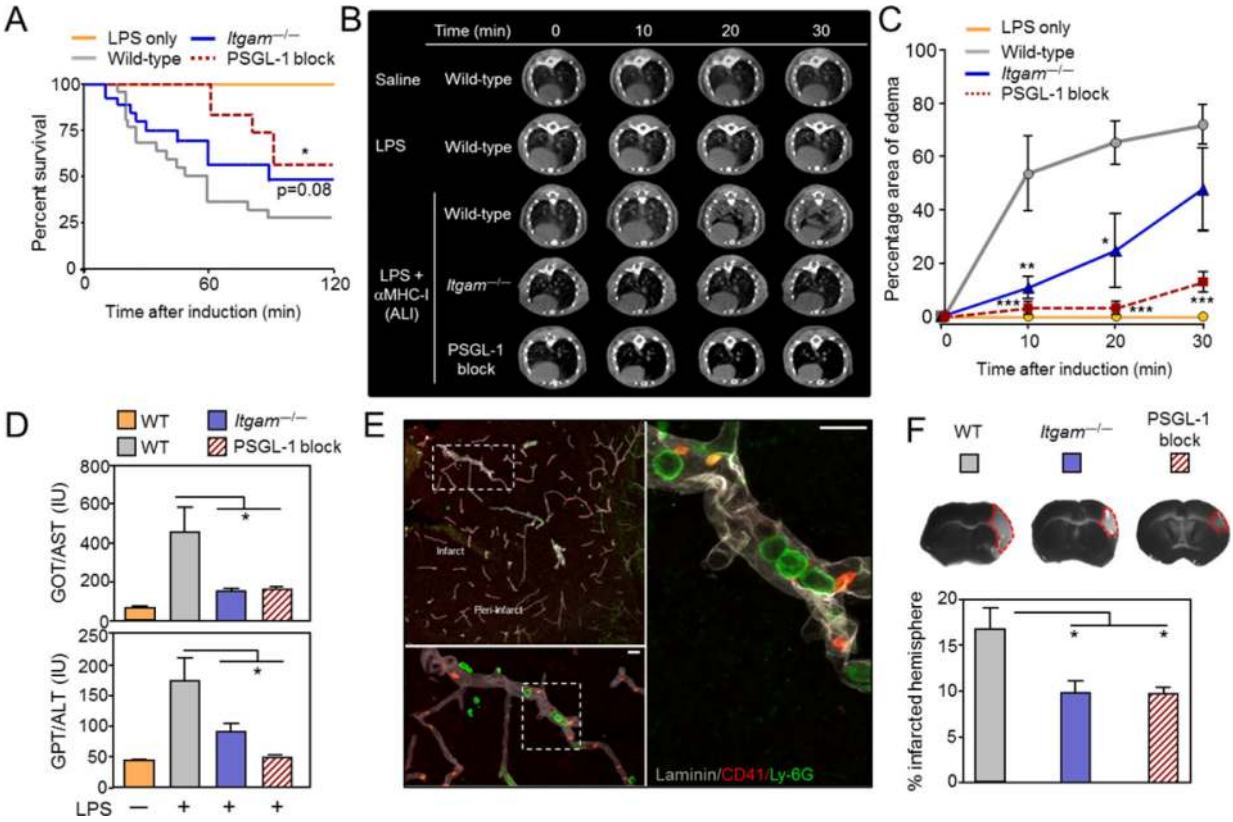

Figure 4. PSGL-1-mediated interactions trigger vascular injury

(**A**) Survival curves of Balb/c mice treated with LPS alone or LPS + anti-MHC-I to induce ALI. Absence of Mac-1 or inhibition of PSGL-1 protect from death; n=5-19 mice. (**B**) Representative axial slices of the thorax of Balb/c mice at different times after induction of ALI. White signal in the pulmonary space identifies edema, which is quantified in (**C**); n=7-8 mice per group. (**D**) Quantification of hepatic injury as levels of AST and ALT transaminases in plasma of the indicated group of mice 24h after treatment with LPS; n=7-11 mice. (**E**) Representative brain sections of wild-type mice 24h after inducing ischemia showing vessels at increasing magnifications, and intravascular neutrophil (Ly6G, green)-platelet (CD41, red) aggregates. Scale bars, 10 μm. (**F**) Percentages of infarcted hemispheres 24h after arterial occlusion in control wild-type mice (WT), mice deficient in Mac-1 (*Itgam*$^{-/-}$) and WT mice after blocking PSGL-1. Images are representative brain sections stained with TTC showing the extent of ischemia as white areas with a red outline; n=5- 8 mice. Bars show mean ± SEM. *, p<0.05; **, p<0.01; ***, p<0.001, ANOVA analysis with Tukey's multigroup test.